SAR Imaging Using SDR

Project for course *Communication Systems Design and Implementation*

Jida Zhang, Hanzhe Guo

Dept. of EE, Tsinghua University

June, 2023

Outline

SAR Imaging

SAR

Synthetic Aperture Radar (SAR) imaging is a radar technique that synthesizes a larger effective antenna aperture by processing data from smaller real antenna apertures. It is also known as Synthetic Aperture Radar or SAR.

The imaging process primarily involves two steps: radar ranging and synthetic aperture synthesis.

- The first step utilizes the radar to transmit and receive signals at a specific location, obtaining range information of the target along the radial direction.
- The second step involves changing the radar's position to acquire range information of the target at different azimuth points, thereby obtaining azimuth information.

SAR Imaging: First Step

The first step is achieved through Frequency Modulated Continuous Wave (FMCW) radar.

FMCW

In FMCW radar, the transmitting end generates a signal with a frequency that varies over time, while the receiving end simultaneously captures the reflected signal.

The simplest FMCW generates a signal with a frequency that linearly changes over time, i.e.,

$$f(t) = c_r t + f_0 - \frac{\mathrm{BW}}{2}, \quad 0 < t < T, \tag{1}$$

where T is the waveform period, f_0 is the carrier frequency, BW is the bandwidth of the sweep, and $c_r = \mathrm{BW}/T$ is the sweep rate.

SAR Imaging: First Step

The FWCM signal $s(t)$ is given by

$$s(t) = \exp\left(j2\pi f(t)t\right) = \exp\left(j2\pi(c_r t + f_0 - \frac{\mathrm{BW}}{2})t\right). \tag{2}$$

Assuming there is a target at a distance d in front of the radar, then the received signal experiences a delay of $\Delta t = \frac{2d}{c}$

$$\begin{aligned} s'(t) &= s(t - \Delta t) \\ &= \exp\left(j2\pi(c_r(t - 2d/c) + f_0 - \frac{\mathrm{BW}}{2})(t - 2d/c)\right). \end{aligned} \tag{3}$$

The mixed signal of $s'(t)$ and $s(t)$ is

$$m(t) = s'(t) \times s^*(t) = A\exp\left(-j4\pi c_r dt/c\right), \tag{4}$$

where $A = \exp(-2f_0 d/c + \mathrm{BW}d/c)$ is a constant.

SAR Imaging: First Step

The frequency information of the mixed signal can be obtained through Fourier transform, resulting in a single peak when there is only one target

$$M(j\omega) = \mathcal{F}(m(t)) = A\delta(\omega - 4\pi c_r d/c). \tag{5}$$

Once the frequency at the peak ω_0 is obtained ($\omega_0 = 4\pi c_r d/c$), the distance from the target to the radar can be calculated

$$\boxed{d = \frac{\omega_0 c}{4\pi c_r}.} \tag{6}$$

SAR Imaging: First Step

Below is a schematic diagram of the transmission, reception, and mixed signal frequencies

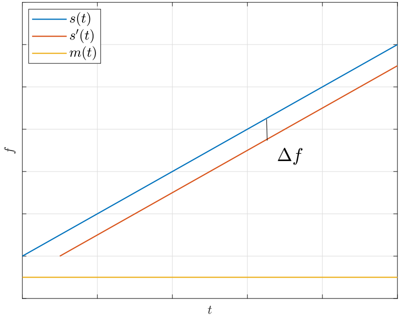

Figure 1: How the frequency of $s(t), s'(t)$ and $m(t)$ changes over time

SAR Imaging: Second Step

Synthetic Aperture

Synthetic aperture refers to the process of moving the radar along the trajectory of the long line array at a constant speed and radiating signals, and performing coherent processing on the received echoes at different positions to obtain a higher resolution imaging result.

- Based on the first step, and the position of the radar needs to be moved, and the received signal needs to be processed by synthetic aperture.
- There are many methods for synthetic aperture, including Range Doppler Algorithm (RDA), Chip Scaling algorithm, Range Migration Algorithm (RMA), etc.
- In this experiment, we use the RMA algorithm.

SAR Imaging: Second Step – RMA Algorithm

The received signal is

$$s(t) = \exp(j2\pi f_0 t + j2\pi c_r t^2), \ -T_s/2 < t < T_s/2. \tag{7}$$

So the result of mixing is

$$s_{\text{IF}}(t) = s(t-t_d)s^*(t) = \exp(-j2\pi f_0 t_d - j2\pi \times 2c_r t \times t_d + j2\pi c_r t_d^2), \tag{8}$$

where $t_d = 2R(x)/c$.
Assuming the target is located at (x_0, y_0), then the distance is

$$R(x) = \sqrt{y_0^2 + (x_0 - x)^2}. \tag{9}$$

SAR Imaging: Second Step – RMA Algorithm

Substituting s_{IF} into Eq. (8), we get

$$s_{\mathrm{IF}}(t) = \exp\left(-j2\pi\frac{f_0 2R(x)}{c} - j2\pi\frac{2c_r t \times 2R(x)}{c} + j2\pi c_r(\frac{2R(x)}{c})^2\right)$$
$$= \exp\left(-j\frac{4\pi}{c}(f_0 + 2c_r t)R(x)\right)\exp\left(j\frac{8\pi c_r}{c^2}R^2(x)\right). \quad (10)$$

The last term is called residual video phase (RVP). To eliminate this term, we expect to multiply the mixed result by $\exp(-j\frac{8\pi c_r}{c^2}R^2(x))$. However, since we do not know $R(x)$ directly, we need to convert it. Note that the frequency offset we get is $f = 4c_r R(x)/c = -2c_r t_d$, so $t_d = -\frac{f}{2c_r}$. Therefore, to eliminate RVP, we only need to multiply by $\exp(-j\pi\frac{f^2}{2c_r})$.

SAR Imaging: Second Step – RMA Algorithm

Assuming the sampling point of each sampling is x_n, the data result after eliminating RVP is

$$s_{\mathrm{IF}}(t) = \exp\left(-j\frac{4\pi}{c}(f_0 + 2c_r t)\sqrt{y_0^2 + (x_0 - x_n - vt)^2}\right). \quad (11)$$

The goal of the second step is to convert the signal into the form $\exp(-j2\pi f_y y_0)\exp(-j2\pi f_x x_0)$, and then use IFFT to obtain an impulse signal at (x_0, y_0).

Defining $2c_r t = f_t$ and s_{IF} turns to

$$S(f_t, x_n) = \exp\left(-j\frac{4\pi}{c}(f_0 + f_t)\sqrt{y_0^2 + (x_0 - x_n - \frac{vf_t}{2c_r})^2}\right). \quad (12)$$

SAR Imaging: Second Step – RMA Algorithm

For convenience, define wave number $K_r = K_{rc} + \Delta K_r$, where $K_{rc} = \frac{4\pi f_0}{c}, \Delta K_r = \frac{4\pi f_t}{c} = -\frac{4\pi BW}{c}, \cdots, \frac{4\pi BW}{c}$, then

$$S(K_r, x_n) = \exp\left(-jK_r\sqrt{y_0^2 + (x_0 - x_n - \frac{vc\Delta K_r}{8\pi c_r})^2}\right). \quad (13)$$

Doing FFT on $S(K_r, x_n)$ over x_n, we get

$$\begin{aligned} S(K_r, K_x) &= \int_{-\infty}^{\infty} S(K_r, x_n) \exp(-j2\pi K_x x_n) \mathrm{d}x_n \quad (14) \\ &= \int_{-\infty}^{\infty} \exp(j\Phi(x_n)) \mathrm{d}x_n, \end{aligned}$$

where

$$\Phi(x_n) = -cK_r\sqrt{y_0^2 + (x_0 - x_n - \frac{vc\Delta K_r}{8\pi c_r})^2} - K_x x_n. \quad (15)$$

SAR Imaging: Second Step – RMA Algorithm

By the principle of stationary phase (POSP), we have $\Phi(\hat{x}_n)$, such that $\frac{\mathrm{d}\Phi(x_n)}{\mathrm{d}x_n}|_{x_n=\hat{x}_n} = 0$.
Therefore, we can write $\Phi(x_n)$ in the form of second-order Taylor expansion (ignoring higher-order terms) $\Phi(x_n) = \Phi(\hat{x}_n) + 0 + \frac{1}{2}\Phi''(\hat{x}_n)(x_n - \hat{x}_n)^2$, and substitute it into Eq. (**??**)

$$\begin{aligned}
S(K_r, K_x) &= \exp(j\Phi(\hat{x}_n)) \int_{-\infty}^{\infty} \exp(j\frac{1}{2}\Phi''(\hat{x}_n)(x_n - \hat{x}_n)^2)\mathrm{d}x_n \\
&= \exp(j\Phi(\hat{x}_n)) \int_{-\infty}^{\infty} \exp(j\frac{1}{2}\Phi''(\hat{x}_n)s^2)\mathrm{d}ds \\
&= \exp(j\Phi(\hat{x}_n))\sqrt{\frac{2\pi j}{\Phi''(\hat{x}_n)}}.
\end{aligned} \tag{16}$$

The last step uses the conclusion $\int_{-\infty}^{\infty} exp(jx^2)\mathrm{d}x = (1+j)\sqrt{\frac{\pi}{2}}$.

SAR Imaging: Second Step – RMA Algorithm

The second term is a real number that only affects the amplitude of the image but not the position, so it can be ignored. Solving $\hat{x}_n$ by setting the first-order derivative to 0, we get

$$\hat{x}_n = x_0 - \frac{vc\Delta K_r}{8\pi c_r} - \frac{K_x y_0}{\sqrt{K_r^2 - K_x^2}}. \tag{17}$$

We finally get the result where x_0 and y_0 are distinguished

$$S(K_r, K_x) = \exp(j(-y_0\sqrt{K_r^2 - K_x^2} - K_x x_0 + \frac{c\Delta K_r K_x v}{8\pi c_r})). \tag{18}$$

The last term can be eliminated by multiplying the opposite phase, and the coefficient of y_0 can be eliminated by using the Stolt interpolation method $\sqrt{K_r^2 - K_x^2} = K_y$, and the final signal is

$$S(K_y, K_x) = \exp(j(-K_y y_0 - K_x x_0)). \tag{19}$$

Pluto-SDR

Software Defined Radio (SDR)

The Pluto-SDR developed by ADALM-Pluto offers advantages such as easy control and wide applicability. We achieve control over it through the MATLAB toolbox.

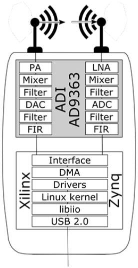

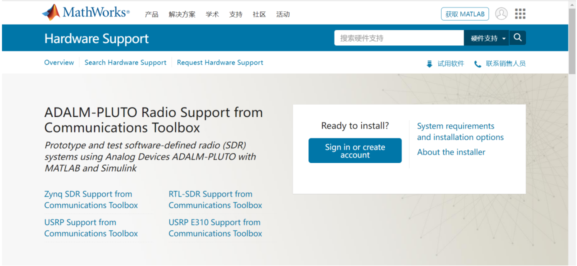

System Block Diagram

The setup mainly includes a computer, a Pluto SDR, and two antennas for transmission and reception. It can be mounted on a bicycle for mobile data collection. The data collected during movement is stored on the computer for subsequent signal processing.

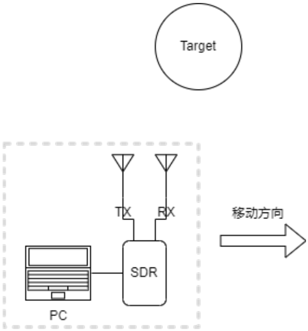

FMCW Parameters

Based on the mobile speed and the size of the SDR reception buffer, a period $T = 1$ ms is chosen. The carrier frequency f_c is selected as 2.4 GHz according to the S11 parameters of the antenna. The final selected parameters are shown in Table 1.

Params	Unit	Value
Sample Rate	MHz	60
Sweep BW	MHz	300
Period	ms	1
Carrier Frequency	GHz	2.45
Sweep Rate	GHz/s	300

Table 1: Main parameters of FMCW

Antenna

The S11 parameters of the antenna were measured using a vector network analyzer, and the results are shown in the graph. It is evident that the values are below -10 dB near the center frequency, meeting the requirements.

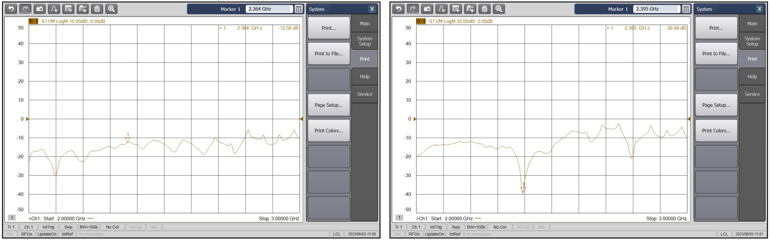

Figure 2: The S11 parameters for the transmit and receive antennas

Antenna

Additionally, there is a strong coupling between the two antennas, as illustrated by the S21 parameters in the graph.

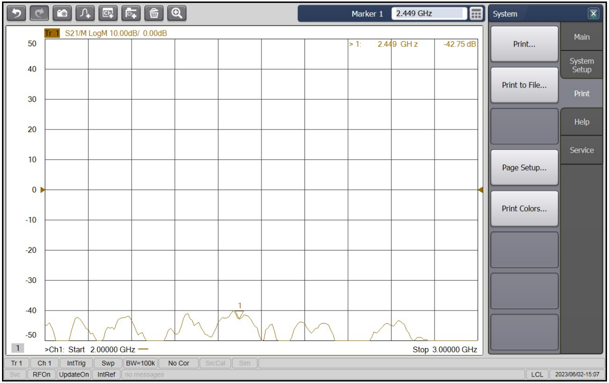

Figure 3: S21

Processing Procedure

Three steps

After acquiring the received signal, the signal processing steps are as follows:

- The first mixing;
- The second mixing;
- Down-sampling.

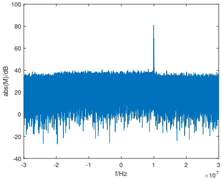

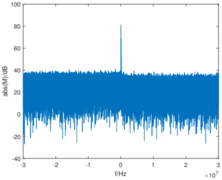

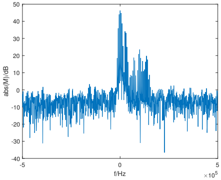

The first mixing

- Unlike the analog approach where the transmitted signal is directly connected to the mixer via a power divider, in our case, we do not know the waveform being transmitted when receiving the signal. Here, we utilize the mutual coupling of the transmit and receive antennas for synchronization.
- We start by using an FMCW signal that sweeps from zero frequency as a reference signal. This reference signal is mixed with the received signal. The resulting mixed frequency spectrum exhibits a main peak, representing the frequency difference between the FMCW signal starting from zero and the received signal.

The first mixing

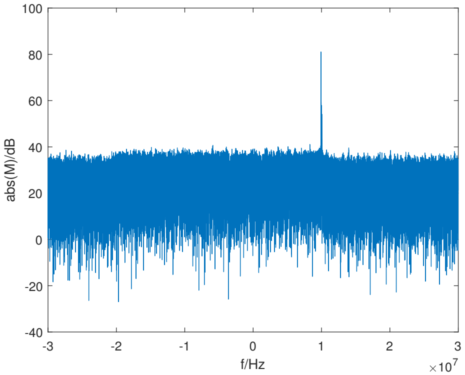

Figure 4: Spectrum of the first mixing signal

The second mixing

As seen in the above graph, the peak is approximately around 10 MHz. Given the bandwidth of 300 MHz, this corresponds to about 1/30 of a period. By cyclically shifting the reference signal, the mixed signal can then appear near zero frequency.

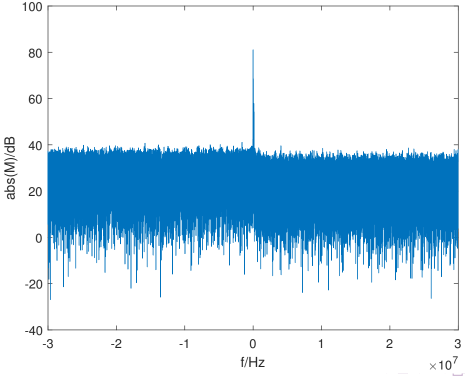

The second mixing

The frequency peak near zero frequency contains the useful signal reflected off objects. Zooming in the region near zero frequency, the result is as shown in the following graph:

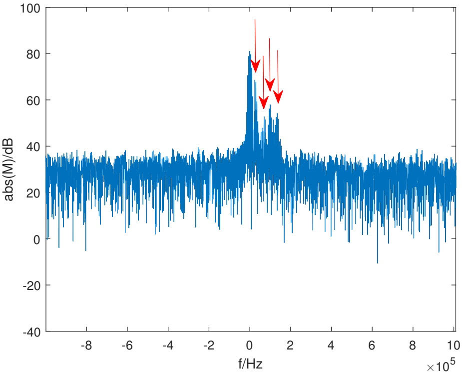

Figure 5: Spectrum of the second mixing signal

Down-sampling

The peaks indicated by the red arrows can provide us with distance information. It's important to note that, due to typical detection distances being on the order of hundreds of meters, and after converting to time differences, the resulting values are generally in the tens of kHz range. Therefore, a sampling frequency of $f_s = 60$ MHz is actually oversampling, and having too many sampled points is not conducive to subsequent SAR algorithm computations.

Therefore, the final step in processing the received signal is downsampling, retaining only a portion of the spectrum near zero frequency. The method involves first applying an anti-aliasing filter, followed by selecting only one point out of every certain number of points and discarding the others. The spectrum after downsampling is shown in the following graph.

Down-sampling

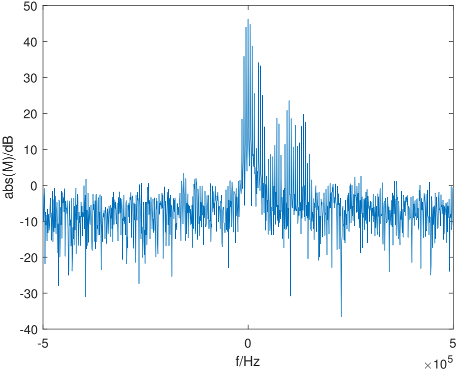

Figure 6: Spectrum of the down-sampled signal

FMCW signal

Using the design parameters, in an ideal scenario, the time-domain waveform and the Short-Time Fourier Transform (STFT) plot are shown below:

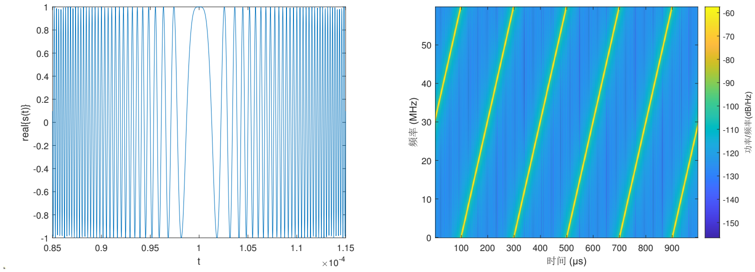

Figure 7: The STFT of ideal FMCW signal

FMCW signal

Taking the data collected in front of the Rohm Building as an example, the actual received signal is shown in the following graph:

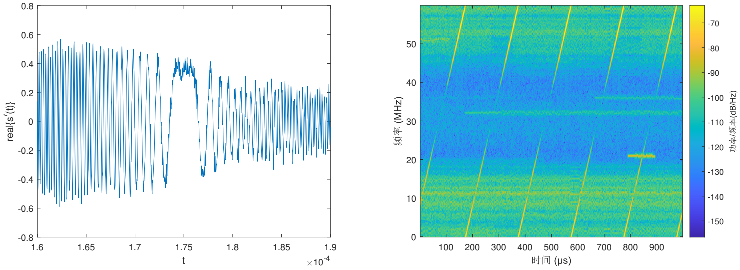

Figure 8: The STFT of actual FMCW signal

Distance Measurement

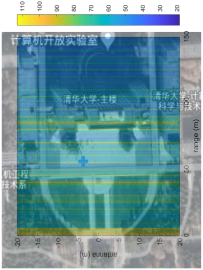

Placing the radar at a specific location for distance measurement, the results show three mean peaks, corresponding to the flagpole, the main building, and the square in front of the main building, respectively. The distances are approximately 45 m, 70 m, and 90 m, respectively, which are consistent with the actual distances.

multiple datasets

After completing the basic verification, to validate the success of the SAR radar imaging we designed, we conducted multiple verification experiments on the campus.

Unlike single-point distance measurement, SAR requires a set of moving sample data to synthesize the aperture. According to the RMA algorithm, compared to single-point distance measurement, we can obtain specific data about the detected object.

Due to equipment limitations, we employed a manual data collection method, simulating uniform motion by walking or cycling. We collected 1000 data points, and the parameters used are detailed in Table 1. Depending on the specific testing target, the distances we covered varied from 40m to 200m.

Imaging for main building

Four buses (three on the left side and one on the right) were parked under the main building, as shown in Figure 9. This arrangement can be used to verify the correctness of our imaging.

Figure 9: Buses in front of main building

Imaging for main building

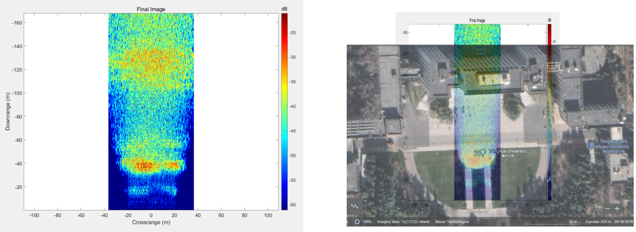

Figure 10: Imaging result

At 40m, a large red shadow appears on the left side, and the red shadow on the right side is smaller, indicating that there are more buses on the left side, which is consistent with reality. In addition, the relative positions of the observation line, buses, and the main building also match the actual situation, indicating the initial successful validation of the algorithm.

Imaging for Rohm Building

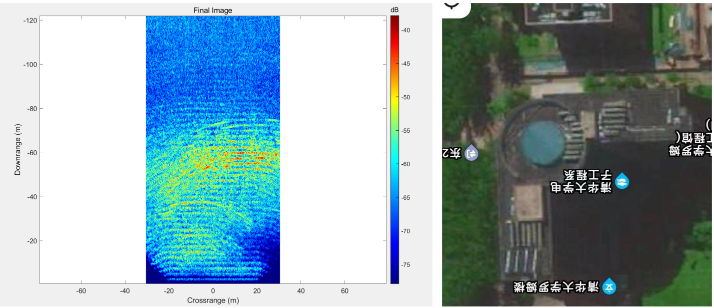

Figure 11: Imaging for Rohm Building

The book-shaped structure of the Rom Building can be observed. However, due to the obstruction of trees along the path, the outline of the Rom Building is not very clear.

Imaging for Island

Using SAR to observe the island in the center of the lake provides a basis for comparing the imaging results under a longer path trajectory (i.e., a larger synthetic aperture). The imaging result is shown in Figure 12:

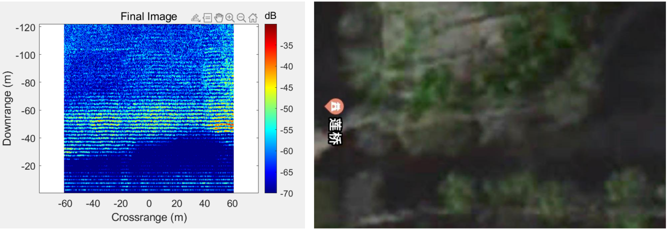

Figure 12: Imaging for Island

Imaging for Island

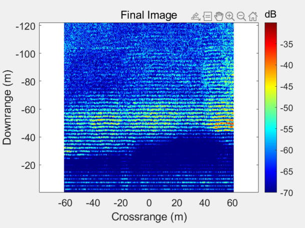

The contour of the island is consistent with the observed image. It's worth noting that, due to a row of willow trees along our path towards the island, while affecting the imaging effect, the clustered shadows of the willow trees can also be seen in the imaging result.

Imaging for Main Building Square

Finally, we returned to the main building and attempted to observe the semicircular structure of the main building's square using SAR with a larger aperture. The imaging result is shown in Figure 13:

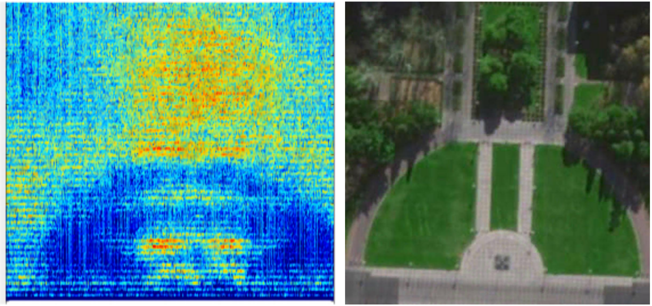

Figure 13: Imaging for Main Building Square

Imaging for Main Building Square

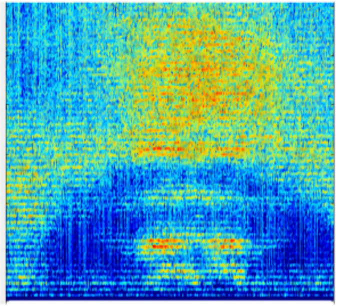

It can be observed that the semicircular structure of the main building's square is clearly imaged. In the more pronounced areas of red shadow, we can observe stone pillars, streetlights, and tree groves.